Measurement of the Vector and Tensor Asymmetries at Large Missing Momentum in Quasielastic ($\vec{e}$, e'p) Electron Scattering from Deuterium

PROCEEDINGS OF SCIENCE

Measurement of the Vector and Tensor Asymmetries at Large Missing Momentum in Quasielastic $(\vec{\mathbf{e}}, \mathbf{e}'\mathbf{p})$ Electron Scattering from Deuterium

Richard G. Milner (for the BLAST Collaboration)[∗†]
Laboratory for Nuclear Science and Department of Physics, MIT, Cambridge, MA 02139, USA
E-mail: milner@mit.edu

We report the measurement of the beam-vector and tensor asymmetries A^V_{ed} and A^T_d in quasielastic $(\vec{e}, e'p)$ electrodisintegration of the deuteron at the MIT-Bates Linear Accelerator Center up to missing momentum of 500 MeV/c. Data were collected simultaneously over a momentum transfer range $0.1 < Q^2 < 0.5$ (GeV/c)^2 with the Bates Large Acceptance Spectrometer Toroid using an internal deuterium gas target, polarized sequentially in both vector and tensor states. The data are compared with calculations. The beam-vector asymmetry A^V_{ed} is found to be directly sensitive to the D-wave component of the deuteron and have a zero-crossing at a missing momentum of about 320 MeV/c, as predicted. The tensor asymmetry A^T_d at large missing momentum is found to be dominated by the influence of the tensor force in the neutron-proton final-state interaction. The new data provide a strong constraint on theoretical models.

23rd International Spin Physics Symposium - SPIN2018 -
10-14 September, 2018
Ferrara, Italy

∗Speaker.
†Published as A. DeGrush *et al.*, Phys. Rev. Lett. **119**, 182501 (2018)

PoS(SPIN2018)026

Understanding the structure and properties of the nucleon-nucleon system is a cornerstone of nuclear physics. Classic studies of the properties of the bound state, (the deuteron) like the magnetic and quadrupole moments, have elucidated the non-relativistic *S*- and *D*-state wave function components. However, modern polarized beams and targets provide new tools to revisit this subject to provide more stringent tests of our understanding. Spin-dependent quasielastic $(\vec{e}, e'p)$ electron scattering from both vector and tensor polarized deuterium provides unique access to the orbital angular momentum structure of the deuteron, which is inaccessible in unpolarized scattering [1]. The combination of a pure, highly polarized gas target internal to a storage ring with an intense, highly polarized electron beam and a large acceptance detector allows the simultaneous measurement of the asymmetries as a function of initial-state proton momentum and momentum transfer. To see the direct effects of the *D*-state, initial-state momenta up to 500 MeV/c are required. Further, nucleon-nucleon correlations with high relative momenta are known to play a significant role in nuclear structure [2]. The tensor force between the neutron and proton can be probed via final-state interaction (FSI) effects in spin-dependent quasielastic $^2\mathrm{H}(\vec{e}, e'p)$ at large initial-state momenta [3, 4]. In this Letter, we report on new measurements of the vector and tensor asymmetries in quasielastic $(\vec{e}, e'p)$ scattering from deuterium over a broad range of kinematics and compare with theoretical calculations.

The deuteron's simple structure enables reliable calculations to be performed in sophisticated theoretical frameworks. These calculations use nucleon-nucleon potentials as input, which show that the ground-state wave function is dominated by the *S*-state at low relative proton-neutron momentum $\mathbf{p}$. The tensor component of the NN interaction generates an additional *D*-state component. Models predict that the $S-$ and $D-$state components strongly depend on $\mathbf{p}$. In the $^2\mathrm{H}(\vec{e}, e'p)$ reaction, energy ν and three-momentum $\mathbf{q}$ are transferred to the deuteron. The cross section can be measured as a function of the missing momentum $\mathbf{p_m} \equiv \mathbf{q} - \mathbf{p_f}$, where $\mathbf{p_f}$ is the measured momentum of the ejected proton.

The cross section can be written in terms of the unpolarized cross section S_0 multiplied by asymmetries diluted by various combinations of the beam's longitudinal polarization h, the target vector polarization P_z, and the target tensor polarization P_{zz} [5] as:

$$\frac{d\sigma}{d\omega d\Omega_e d\Omega_{pn}^{CM}} = S_0 \left[1 + P_z A_d^V + P_{zz} A_d^T + h \left(A_e + P_z A_{ed}^V + P_{zz} A_{ed}^T \right) \right] .$$

In the Born approximation A_e, A_d^V, and A_{ed}^T are all zero. In a purely *S*-state A_d^T is also zero but will vary from zero as *D*-state contributions become important providing a measure of the tensor component of the NN interaction. Similarly, A_{ed}^V will vary from hP_z as *D*-state contributions become significant.

Previous measurements of the asymmetries A_d^T up to $p_m = 150$ MeV/c [6] and of A_{ed}^V up to $p_m = 350$ MeV/c [7] were carried out at NIKHEF. These pioneering measurements did not have the kinematic reach to observe the effects of the *D*-state in A_{ed}^V or the FSI effects in A_d^T.

Our experiment was carried out with the Bates Large Acceptance Spectrometer Toroid (BLAST) [8, 9]. The BLAST experiment; including details on the detector, the South Hall Ring (SHR) of the MIT-Bates Linear Accelerator Center, the longitudinal polarized electron beam, the atomic beam source [10] (ABS) that produced the vector and tensor polarized deuterium, and the experimental operation; has been described extensively in the cited references and will not be repeated here.

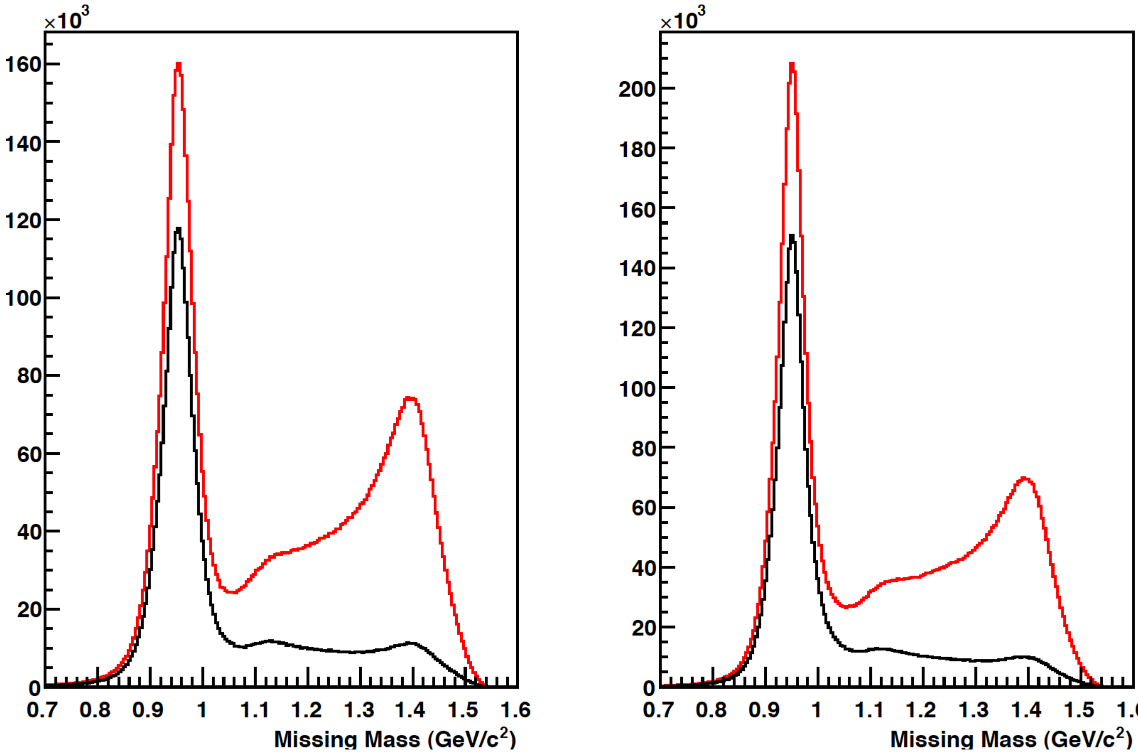

Figure 1: Histograms (color online) of the yields versus missing mass for target spin angle $\approx 31^\circ$ without (red) and with (black) Čerenkov cuts for $0.1 < Q^2 < 0.5$ (GeV/c)^2 for *opposing* (left) and *same* (right) sector kinematics.

The target spin states were switched every 5 minutes. The longitudinal beam polarization was reversed every injection cycle and was monitored continuously using a Compton back-scattering polarimeter. The average polarization was $h = 0.6558 \pm 0.007(\mathrm{stat}) \pm 0.04(\mathrm{sys})$.

The data were taken in two separate running periods and acquired simultaneously with the BLAST measurements of G_E^n [11] and T_{20} [12]. The average target spin angles were $31.3^\circ \pm 0.43^\circ$ and $47.4^\circ \pm 0.45^\circ$ with respect to the beam axis for the two run periods. The target spin angle was in the horizontal plane pointing into the left sector and was determined using elastic electron-deuteron scattering [12]. Electrons scattered into the right (left) sector delivered momentum transfer predominantly parallel (perpendicular) to the target spin vector, so-called *same sector* (*opposing sector*) kinematics.

The average product of beam and target polarization was determined from measuring A_{ed}^V in the $^2\vec{\mathrm{H}}(\vec{e}, e'p)$ reaction in the quasielastic limit (low missing momentum, $p_m < 0.1$ GeV/c) where the reaction is close to elastic ep scattering. The results were $hP_z = 0.5796 \pm 0.0034(\mathrm{stat}) \pm 0.0054(\mathrm{syst})$ in the first run and $0.5149 \pm 0.0043(\mathrm{stat}) \pm 0.0054(\mathrm{syst})$ in the second run. In parallel, hP_z was similarly determined from the quasielastic $^2\vec{\mathrm{H}}(\vec{e}, e'n)$ reaction and was found to be in good agreement.

The target tensor polarizations were determined from fits to the elastic electron-deuteron observable T_{20} [12] using parameterizations to previous data [13]. The results were $P_{zz} = 0.683 \pm 0.015 \pm 0.013 \pm 0.034$ and $0.563 \pm 0.013 \pm 0.023 \pm 0.028$, where the three uncertainties are statistical, systematic, and due to the parametrization of T_{20}, in that order.

The event selection is described in detail in the theses of A. Maschinot [14] and A. DeGrush [15]. Briefly, electron-proton coincidence events were selected using a series of PID, timing, and vertex cuts. Events were chosen with two oppositely charged (curvature) tracks in opposing sectors. The Čerenkov detectors were used to distinguish electrons from π^- and time of flight was used to select proton events while rejecting events with π^+ or a deuteron. To ensure that the two particles came from the same event, a cut was placed on the relative separation of their vertices in the target $|z_p - z_e| < 5$ cm. Once these events were selected each track's kinematic variables, $(p_e, \theta_e, \phi_e, z_e)$ for the electron and $(p_p, \theta_p, \phi_p, z_p)$ for the proton, were used to determine the variables (Q^2, p_m, m_m). The quasielastic events were selected by placing a 2.5σ cut around the peak of the missing mass spectrum (see Fig. 1) representing the remaining neutron.

After background subtraction and correcting for false asymmetries determined from the empty target runs the resulting yield in the various Q^2 and p_m bins could be determined for the combinations of beam and deuterium vector and tensor orientations (±1, ±1 or 0, +1 or -2) for which data was collected. The charge normalized yields or event rates could be combined to give the desired asymmetries. For this paper:

$$\begin{aligned} S_0 &= \frac{1}{6}[R(1,1,1)+R(-1,1,1)+R(1,-1,1)+R(-1,-1,1)+2R(1,0,-2)+2R(-1,0,-2)] \\ A^V_{ed} &= \frac{1}{4hP_zS_0}[R(1,1,1)-R(-1,1,1)-R(1,-1,1)+R(-1,-1,1)] \\ A^T_d &= \frac{1}{12P_{zz}S_0}[R(1,1,1)+R(-1,1,1)+R(1,-1,1)+R(-1,-1,1)-2R(1,0,-2)-2R(-1,0,-2)]\,, \end{aligned} \tag{1}$$

where $R(h, P_z, P_{zz})$ is the charge normalized yield or event rate for each spin orientation combination.

Radiative corrections to the asymmetries were calculated using the MASCARAD code [16] and all found to be less than 1%. Thus, no corrections were applied to the asymmetries but a systematic uncertainty of ±1% was included. Background arose predominantly from beam collisions with the target cell wall. Estimates for this rate were made by acquiring data with and without gas in the target cell. Background was subtracted on a bin-by-bin basis and increased from a typical value of < 1% at low p_m to of order 10% at the highest p_m.

The beam-vector asymmetries A^V_{ed} for the runs with the two target spin orientations are shown in Fig. 2. The data are shown in *same sector* and *opposing sector* kinematics as a function of the missing momentum p_m for momentum transfers $0.1 < Q^2 < 0.5$ (GeV/c)^2. The values of p_m extend up to about 500 MeV/c and the data are compared with theoretical calculations based on the model of Arenhövel, Leidemann, and Tomusiak [17]. The model was calculated for the kinematics of the experiment folding in the detector acceptances and efficiencies in a comprehensive GEANT simulation. The curves shown in each plot correspond to a plane-wave Born approximation (PWBA) which includes the coupling to the neutron, a PWBA with final state interactions (FSI) and a full calculation beyond PWBA+FSI including the effects of meson-exchange currents (MEC), isobar configurations (IC) and relativistic corrections (RC). The two-body wave functions needed for the calculation of the observables are based on the realistic Bonn potential [18], which is defined in purely nucleonic space. The theoretical calculations were found to be insensitive to the choice of

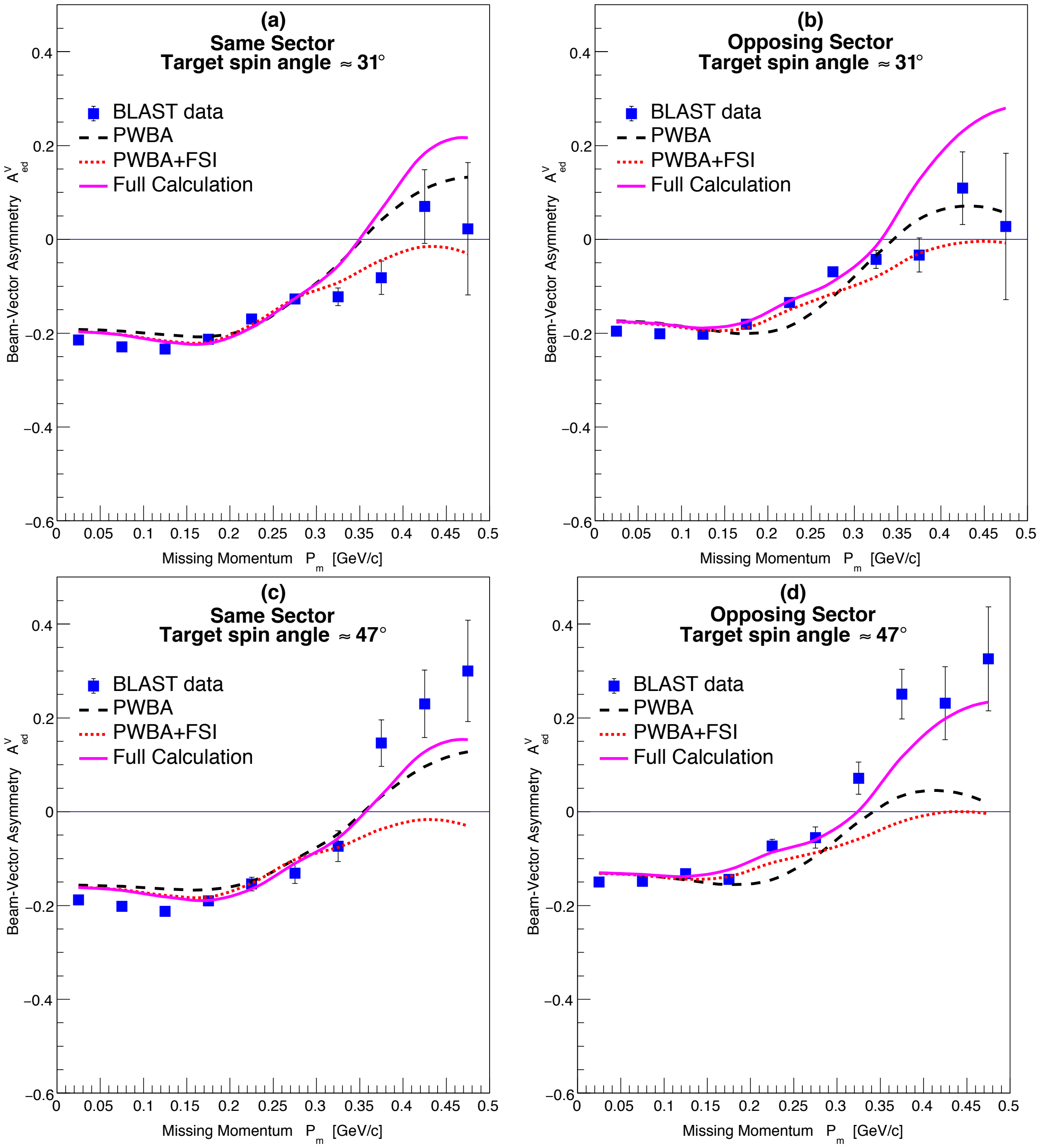

Figure 2: Beam vector asymmetries A^V_{ed} for $0.1 < Q^2 < 0.5$ (GeV/c)^2 vs. p_m. Panels (a) and (c) refer to *same sector* kinematics for target spin angles $\approx 31^\circ$ and $\approx 47^\circ$. Panels (b) and (d) refer to *opposing sector* kinematics for the same target spin angles.

different realistic potentials (*e.g.* Reid [19], Paris [20], Argonne V14 and V18 [21]). The treatment of MEC, IC, and RC is done consistently according to [17, 22].

At the $p_m = 0$ limit the opposing sector asymmetries are directly proportional to the product hP_z, a key parameter that has been determined with better than 1% absolute accuracy. The target vector polarization P_z is directly related to the polarization P of the proton or neutron bound in the deuteron such that [23]

$$P = \sqrt{\frac{2}{3}} P_z (P_S - \frac{1}{2} P_D) \ , \qquad (2)$$

where P_S and P_D are the S- and D-state probabilities of the deuteron, respectively. This illustrates the fact that the polarization of a nucleon in the D-state is opposite to that of a nucleon in the S-state, as expected from angular momentum considerations for a $J^\pi = 1^+$ system like the deuteron. The present results for the A^V_{ed} asymmetries show for the first time the evolution going from the S-state to the D-state in momentum space. The A^V_{ed} are constant up to about $p_m = 150$ MeV/c which is consistent with an S-state, then as p_m increases, the presence of the D-state lowers the proton polarization in the deuteron until it changes sign when $P_D \geq 2P_S$.

Figure 2 shows that the experimental asymmetries A^V_{ed} are in good agreement with the full theoretical calculations over a wide range of Q^2 and p_m. The only previous measurement of A^V_{ed} was carried out in perpendicular kinematics at NIKHEF [7] up to p_m of about 300 MeV/c, although with limited statical precision after 200 MeV/c. The BLAST data in the region of p_m around 200 MeV/c, where the S- and D-states strongly interfere, are very well described by the full theoretical calculation in contrast to the claim in [7] where the data suggested an underestimation by the theory. The A^V_{ed} asymmetries directly relate to the deuteron momentum distribution for the $M_d = \pm 1$ spin states. It has been pointed out [24] that the $M_d = 1$ momentum distribution has a zero around 300 MeV/c, which in a simple picture can be related to the dimensions of the toroidal shape of the density distribution. The Fourier transform of the deuteron density calculated in the model of Ref. [24] yields a zero at 320 MeV/c for the $M_d = 1$ momentum distribution [15], which is where the A^V_{ed} asymmetries in Fig. 2 have their zero-crossings. This zero crossing was also predicted by Jeschonnek and Donnelly [25] using an improved treatment of the non-relativistic reduction of the electromagnetic current operator.

Figure 3 shows the tensor analyzing powers A^T_d as a function of p_m for the same kinematics and target spin orientations as that of Fig. 2, and compared also with the same theoretical model folded with the detector acceptances and efficiencies. Just as for A^V_{ed} the only previous measurement of A^T_d was carried out in parallel kinematics at NIKHEF [6] up to p_m of only 150 MeV/c with limited statistics. The BLAST A^T_d data extend up to p_m = 500 MeV/c and for the first time into the region where the D-state dominates over the S-state. As expected, where the S-state dominates, the A^T_d are small and well described by the theoretical calculations, including the simple PWBA. Beyond about p_m = 150 MeV/c A^T_d grows, indicating the effect of the tensor polarization. The PWBA calculations show that the sign is different for the A^T_d in *same sector* and *opposing sector* kinematics.

As shown in Fig. 3, in contrast to the vector asymmetries A^V_{ed}, the tensor asymmetries A^T_d are significantly modified by the effects of the FSI for $p_m \geq 150$ MeV/c. In *same sector* kinematics, the effects of FSI bring the A^T_d calculations into reasonable agreement with the present data. In *opposing sector* kinematics, the effects of the FSI are also sizable but not sufficient to agree with the data; the effects of MEC and IC contribute equally after FSI to produce the full calculations of Fig. 3. The kinematic reach of the BLAST data is such that the proton-neutron interaction is sampled via the FSI over a large spatial range: from short distances, where the nucleons are expected to overlap, to long distances where the interaction is dominated by one-pion-exchange. The A^T_d data at $p_m \geq 250$ MeV/c are particularly sensitive to the tensor part of the interaction at

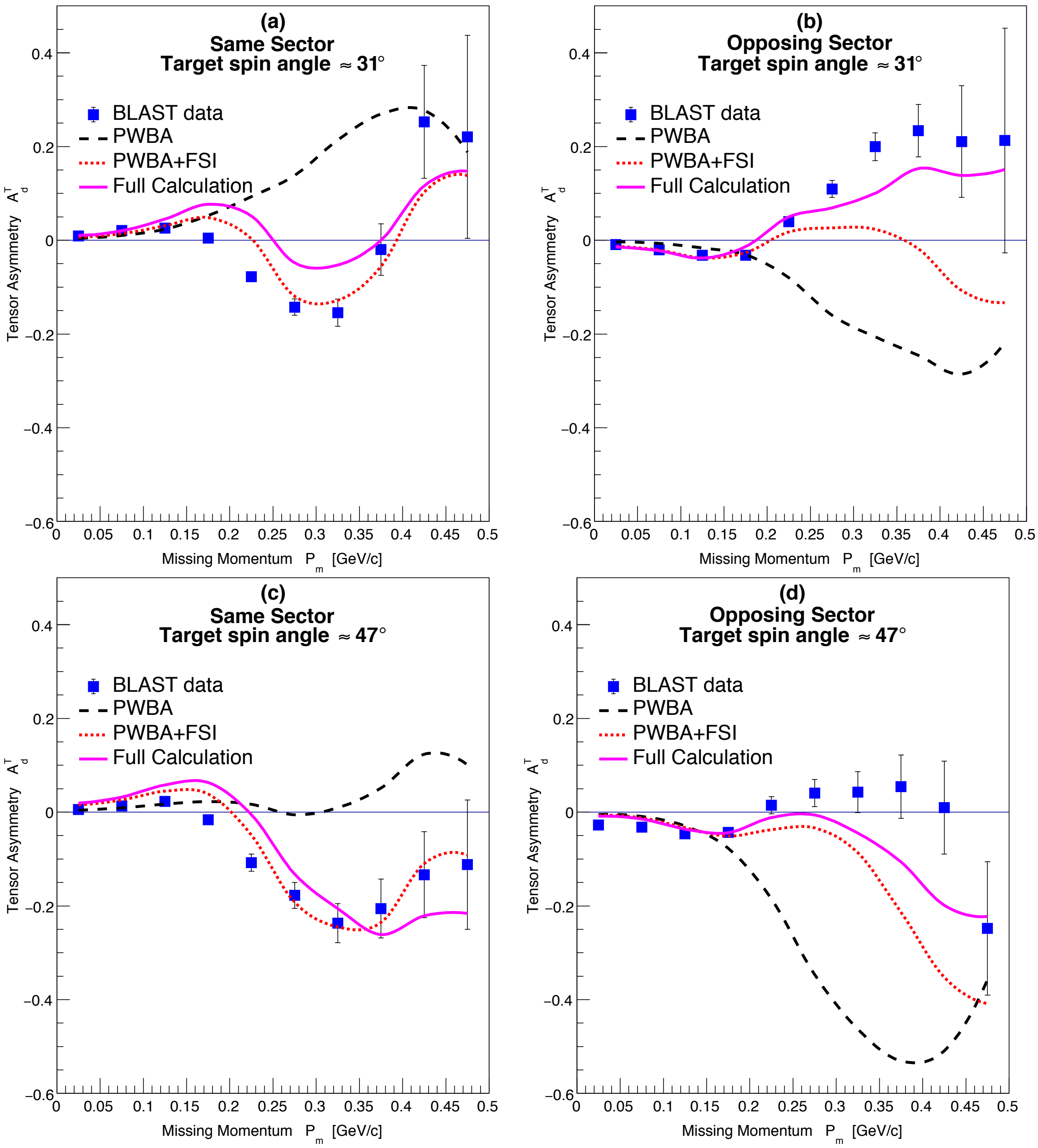

Figure 3: Tensor asymmetries A_d^T for $0.1 < Q^2 < 0.5$ (GeV/c)^2 vs. p_m. Panels (a) and (c) refer to *same sector* kinematics for target spin angles $\approx 32°$ and $\approx 47°$. Panels (b) and (d) refer to *opposing sector* kinematics for the same target spin angles.

short distances, where it has significant model dependence [24]. It is to be noted that the theoretical model used here works well, given that it is mainly based on nucleon degrees of freedom.

We have presented data for the vector A^V_{ed} and tensor A^T_d spin asymmetries from the deuteron for $0.1 < Q^2 < 0.5$ (GeV/c)^2. The asymmetries were mapped out for quasielastic kinematics $(\vec{e}, e'p)$ over a range of p_m up to $\sim$ 500 MeV/c. The data were taken using an internal deuterium gas target polarized in both vector and tensor spin states that minimized systematic errors. This was done simultaneously with precise measurements of the elastic [12] and the $(e, e'n)$ [11] channels that also permitted measurements of P_{zz} and P_z. The new data are in good agreement with theoretical calculations and provide a strong constraint on our understanding of deuteron structure and the tensor force between a neutron and a proton. The D-state contribution is clearly evident in both asymmetries as p_m increases and highlights the importance of measurements at large p_m. The tensor asymmetries with same and opposing sector kinematics probes the proton-neutron interaction over a large spatial range. These results and approach are important for future theoretical calculations and experiments that study the deuteron and details of the proton-neutron interaction.

Acknowledgments

We thank the staff at the MIT-Bates Linear Accelerator Center for the high quality electron beam and their technical support. We thank H. Arenhövel for many enlightening discussions. This work has been supported in part by the US Department of Energy Office of Nuclear Physics and by the National Science Foundation.

References

[1] W.U. Boeglin, J. Phys. Conf. Ser. **543** 012011, (2014).

[2] O. Hen, G. Miller, E. Piasetzky and L.B. Weinstein, arXiv: 1611.09748, to be published in Reviews of Modern Physics.

[3] S. Jeschonnek and J.W. Van Orden, Phys. Rev. **C95**, 044001 (2017).

[4] M. Mayer *et al.*, Phys. Rev. **C95**, 024005 (2017)

[5] H. Arenhövel, W. Leidemann, and E.L. Tomusiak, Phys. Rev. **C46**, 455 (1992).

[6] Z.L. Zhou *et al.*, Phys. Rev. Lett. **82**, 687 (1999).

[7] I. Passchier *et al.*, Phys. Rev. Lett. **88**, 102302 (2002).

[8] D.K. Hasell *et al.*, Nucl. Instr. and Meth. **A603**, 247 (2009).

[9] D.K. Hasell *et al.*, Ann. Rev. Nucl. Sci. **61**, 409 (2011).

[10] D. Cheever *et al.*, Nucl. Instr. and Meth. **A556**, 410 (2006).

[11] E. Geis *et al.* (The BLAST Collaboration), Phys. Rev. Lett. **101**, 042501 (2008).

[12] C. Zhang *et al.* (The BLAST Collaboration), Phys. Rev. Lett. **107**, 252501 (2011).

[13] D. Abbott *et al.*, Eur. Phys. J. **A7**, 421 (2000).

[14] A. Maschinot, Ph.D. thesis, MIT (2005), http://hdl.handle.net/1721.1/34390.

PoS(SPIN2018)026

[15] A. DeGrush, Ph.D. thesis, MIT (2010), http://hdl.handle.net/1721.1/62644.

[16] A. Afanasev, I. Akushevich, and N. Merenkov, Phys. Rev. **D64**, 113009 (2001).

[17] H. Arenhövel, W. Leidemann, and E.L. Tomusiak, Eur. Phys. J. **A23**, 147–190 (2005).

[18] R. Machleidt, K. Holinde, Ch. Ester, Phys. Rep. **149**, 1 (1987).

[19] R. Reid, Ann. Phys. **50**, 411 (1968).

[20] M. Lacombe *et al.*, Phys. Rev. **C21** 861 (1980).

[21] R. Wiringa, V.G.J. Stoks, and R. Schiavilla, Phys. Rev. **C51** 38 (1995).

[22] F. Ritz, H. Goller, T. Wilbois, H. Arenhovel, Phys. Rev. **C55**, 2214 (1997).

[23] H. Arenhövel, W. Leidemann, and E.L. Tomusiak, Z. Phys. Rev. **A331**, 123–138 (1988).

[24] J.L. Forest *et al.*, Phys. Rev. **C54**, 646 (1996).

[25] S. Jeschonnek and T.W. Donnelly, Phys. Rev. **C57**, 2438 (1998).

PoS(SPIN2018)026